The boson peak of deeply cooled confined water reveals the existence of a low-temperature liquid-liquid crossover

Antonio Cupane, Margarita Fomina, and Giorgio Schirò

Citation: The Journal of Chemical Physics **141**, 18C510 (2014); doi: 10.1063/1.4895793
View online: http://dx.doi.org/10.1063/1.4895793
View Table of Contents: http://scitation.aip.org/content/aip/journal/jcp/141/18?ver=pdfcov
Published by the AIP Publishing

The boson peak of deeply cooled confined water reveals the existence of a low-temperature liquid-liquid crossover

Antonio Cupane,[1,a)] Margarita Fomina,[1] and Giorgio Schirò[2]
[1]*Department of Physics and Chemistry, University of Palermo, via Archirafi 36, 90123 Palermo, Italy*
[2]*CNRS - Institut de Biologie Structurale, 71 avenue des Martyrs, 38000 Grenoble, France*

(Received 15 July 2014; accepted 4 September 2014; published online 23 September 2014)

The Boson peak of deeply cooled water confined in the pores of a silica xerogel is studied by inelastic neutron scattering at different hydration levels to separate the contributions from matrix, water on the pore surfaces and "internal" water. Our results reveal that at high hydration level, where the contribution from internal water is dominant, the temperature dependence of the Boson peak intensity shows an inflection point at about 225 K. The complementary use of differential scanning calorimetry to describe the thermodynamics of the system allows identifying the inflection point as the signature of a water liquid-liquid crossover. © *2014 AIP Publishing LLC*. [http://dx.doi.org/10.1063/1.4895793]

I. INTRODUCTION

Water is one of the most studied systems but, at the same time, its physical behavior is not fully understood, yet. A large number of anomalies characterize water physical properties, at both low and high temperature. In particular, low temperature liquid water (the so-called supercooled state) is known to exhibit many anomalous behaviors compared to its crystalline counterparts, such as the temperature dependence of thermal conductivity and specific heat. Different scenarios have been proposed to rationalize the origin of such anomalies;[1–4] in particular, a recent proposal links the water anomalies to the existence of a second critical point of water al low temperature, originally predicted by molecular dynamics (MD) simulations.[5] The signature of the presence of such point has been identified in the crossing temperature (about 225 K at atmospheric pressure) separating two phases of liquid water, a low density liquid (LDL) phase below 225 K and a high density liquid (HDL) phase above 225 K, as more recently confirmed by experiments and simulations on bulk water,[6] nano-confined water[7–11] and on protein hydration water.[12,13] However, other MD simulations[14,15] and experimental evidences[16–18] seriously questioned the hypothesis of a liquid-liquid phase transition (LLPT), thus revealing that a general agreement about the existence and, if any, the origin of a liquid-liquid crossover is not reached yet.

One of the characteristic features of supercooled water, analogously to glasses and amorphous materials, is the presence of low-frequency modes revealed by inelastic neutron scattering, x-ray scattering and Raman scattering in the energy range 2–10 meV (the so-called Boson peak), where the vibrational density of states g(E) shows an excess over the $g(E) \sim E^2$ law predicted by the Debye model. Many hypotheses have been proposed to explain the physical mechanisms giving rise to the Boson peak, but a comprehensive understanding has proved elusive. In a recent MD study,[19] Stanley and collaborators investigated the origin of the Boson peak in TIP4P/2005 water and found that its onset in supercooled bulk water when temperature is lowered below 225 K coincides with the crossover to a predominantly low-density-like liquid. This behavior was found to be in agreement with some older preliminary experimental data on deeply cooled nano-confined water[20,21] and with more recent data and analysis by the same group.[22]

In this paper, we explored the temperature dependence of the boson peak of supercooled water in order to search for a possible experimental evidence of the LLPT hypothesis. We used a nanoporous silica xerogel matrix to confine water and thus enter the deeply supercooled region. Indeed, it has been shown[23–25] that water confined in such matrices remains liquid at temperatures much lower than the homogeneous nucleation temperature (about 235 K at atmospheric pressure) and thus can be used to explore the properties of liquid water in the so-called "no man's land." Moreover, the hydration level of this kind of matrices can be easily tuned, thus allowing estimating the contribution from matrix and the effect of water interaction with matrix inner surfaces, as detailed in Secs. II and III.

We used inelastic neutron scattering to measure the water spectrum in the Boson peak region in the temperature range 100–280 K. We also complemented the neutron experiments with differential scanning calorimetry (DSC) data on the very same samples, in order to characterize the thermodynamics of water and to detect possible phase transitions in the temperature range investigated.

II. MATERIALS AND METHODS

A. Samples

Silica xerogels were obtained from the alcoxide precursor tetramethylortosilicate through hydrolysis and polycondensation, following the procedure described in Ref. 26. Xerogels consist of a disordered, porous, 3D SiO_2 matrix; within the pores of the matrix (characterized by a broad pore size distribution with average value of about 20 Å[24]) water is confined. After suitable ageing the xerogel samples were crunched to obtain powders whose hydration $h = [gr\ H_2O]/[gr\ SiO_2]$ was

a)E-mail: antonio.cupane@unipa.it

controlled gravimetrically. Three samples have been investigated in this study at hydration levels h = 0.42, 0.19, and 0.05. This last sample was obtained after prolonged vacuum dehydration at 50 °C and was used to obtain the contribution of the "dry" silica matrix. On the other hand, the h = 0.19 sample allows investigating the properties of water mainly interacting with the pore walls, while the h = 0.42 sample gives information also on the internal water.

B. Differential scanning calorimetry

DSC measurements were performed using a Diamond DSC Perkin–Elmer calorimeter equipped with a Cryofill device using liquid nitrogen as a cold source. Indium was used as a standard to calibrate temperature and heat flow. Heat flow error is 0.05 mW. Samples (about 60 mg) were sealed in steel pans; an empty pan was used as reference. Samples were first cooled from room temperature to 120 K at a rate of 5 K/min, mimicking the cooling rate typical of neutron scattering experiments. Calorimetric upscans from 120 to 310 K were measured with a heating rate of 20 K/min.

Baselines, measured at the same scan rate with no pans in the furnace, were subtracted from the measured thermograms.

C. Neutron scattering

1. Measurements

Inelastic neutron scattering (INS) experiments were performed at the time-focusing time-of-flight spectrometer IN6 (Institut Laue-Langevin, Grenoble, France) with an incident wavelength $\lambda = 5.1$ Å and an energy resolution of 70 μeV FWHM. The setting allows to access the momentum transfer range $0.3 < Q < 2$ Å^{-1}. The inelastic spectra S(Q = 1.8 Å^{-1}, E), where E denotes the exchanged energy, were obtained by binning all the measured spectra in the interval $1.6 < Q < 2.0$ Å^{-1}. In view of the relation between energy and momentum transfer ranges in a time-of-flight spectrometer, the choice of this Q region allows to explore the largest energy range accessible. Given the large incoherent cross section of hydrogen, the (coherent + incoherent) contributions from Si and O atoms and the coherent contribution of H atoms were neglected so that the measured inelastic spectra were considered to arise only from the incoherent scattering of hydrogen atoms.

2. Xerogel matrix contribution

The pore walls of the investigated silica xerogels are "decorated" by Si-OH groups that contribute to the total scattered intensity. The contribution has been estimated by measuring the scattering signal of a dry sample (h = 0.05) at 100, 189, 238, and 277 K (Figure 1, upper panel). As shown in Figure 1 (middle panel), all the spectra in the investigated temperature range can be rescaled with a single factor and the temperature dependence of the scaling factor is linear (Figure 1, lower panel). The shape of the matrix spectrum has been then approximated with a heuristic function and rescaled with the parameters of the linear temperature dependence (Figure 1, lower panel) to calculate the matrix contribution to the spectra of hydrated samples. From Figure 1 it can be appreciated also that the matrix contribution shows an almost negligible, if any, vibrational excess around 2–5 meV, i.e., in the energy region of the boson peak.

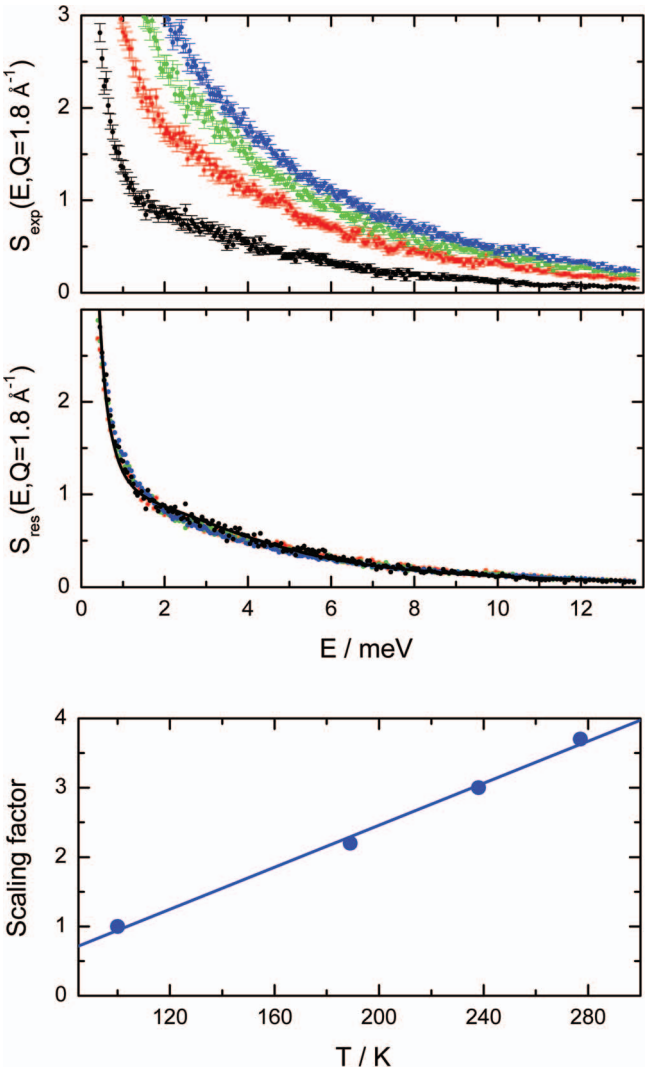

FIG. 1. (Upper panel) Dynamic structure factor of silica matrix; from bottom to top: T = 100 K (black), 189 K (red), 238 K (green), and 277 K (blue). (Middle panel) Rescaled dynamic structure factor of silica matrix with fit (black line). (Lower panel) Temperature dependence of scaling factor and linear fit.

3. Analysis of inelastic spectra

From the physical point of view, the measured inelastic spectra (typical examples are reported in Figure 2) were considered to arise, besides the matrix contribution, from the sum of the following contributions:

1. An elastic contribution arising from nuclei that are at rest in the time window of the experiment and given by a Dirac delta function convoluted with the experimental resolution; in view of the energy resolution used in our experiment (~70 μeV FWHM) the elastic contribution is essentially zero for E > 0.1 meV.

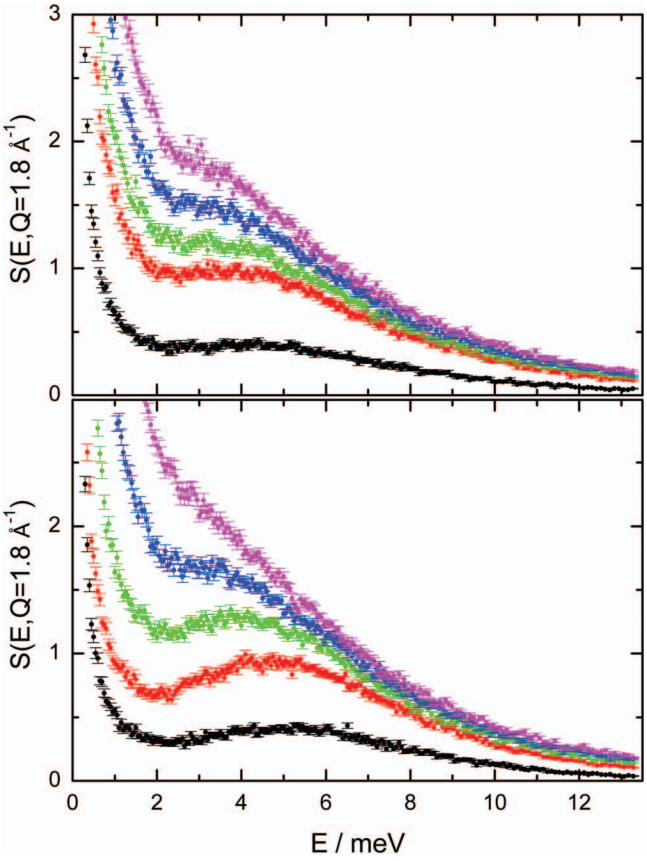

FIG. 2. (Upper panel) Dynamic structure factor of silica xerogel at h = 0.19; from bottom to top: T = 105 K (black), T = 195 K (red), T = 215 K (green), T = 238 K (blue), and T = 255 K (magenta). (Lower panel) Dynamic structure factor of silica xerogel at h = 0.42; from bottom to top: T = 100 K (black), T = 187 K (red), T = 215 K (green), T = 235 K (blue), and T = 257 K (magenta).

2. A quasi-elastic contribution arising from diffusive-like translational and rotational motions occurring in the picoseconds-to-nanosecond time scale. In our approach the analysis of this contribution remains heuristic and is performed with two Lorentzian functions. Note that at temperatures below 180 K the quasi-elastic contribution is almost absent and that, above 180 K, its amplitude and width increase monotonically with temperature (see Figure 6).
3. An inelastic contribution arising from low frequency collective vibrations (the so-called Boson peak (BP); for a discussion on the physical origin of the BP in supercooled water and in deeply cooled confined water see, e.g., Refs. 19 and 22 and references therein). As already proposed in the literature,[27] we account for this contribution with an asymmetric lognormal term.

The function used to analyze the experimental spectra reported here has the following form:

$$S_{\mathrm{exp}}(E, Q = 1.8\,\text{Å}^{-1}) = M(E) + \frac{1}{\pi}\cdot\frac{A_1\gamma_1}{E^2+\gamma_1^2} + \frac{1}{\pi}\cdot\frac{A_2\gamma_2}{E^2+\gamma_2^2} + \frac{A_3}{\sqrt{2\pi}\sigma_{BP}E}\cdot\exp\left[\frac{-(E_{BP}-\ln E)^2}{2\sigma_{BP}^2}\right], \quad (1)$$

where M(E) accounts for the matrix contribution, as described above. Note that the term M(E) contains no adjustable parameters since its amplitude depends on the sample hydration level but not on temperature. A_1, γ_1, A_2, and γ_2 are the amplitudes and halfwidths, respectively, of the two Lorentzian terms L_1 and L_2 used to describe the quasi-elastic contribution; σ_{BP} and E_{BP} are the width and position, respectively, of the asymmetric lognormal term that describes the BP shape. The fitting is performed in the energy range $0.1 < E < 15$ meV, where the tail of the elastic peak (resolution function) can be neglected. The Debye-Waller factor arising from harmonic vibrations is included implicitly in the amplitudes of the various terms in Eq. (1); it will be considered explicitly only in the derivation of the density of states (see below). The inelastic spectra were analyzed with a FORTRAN 95 code based on the Minuit minimization routine released by the CERN computing group (*lcgapp.cern.ch/project/cls/work-packages/mathlibs/minuit/index.html*).

From the lognormal term we obtain the vibrational density of states (VDOS), g(E), according to

$$g(E) \sim \frac{E\cdot\frac{A_3}{\sqrt{2\pi}\sigma_{BP}E}\cdot\exp\left[\frac{-(E_{BP}-\ln E)^2}{2\sigma_{BP}^2}\right]}{n(E,T)\cdot DW(T)}, \quad (2a)$$

$$n(E,T) = \frac{1}{\exp\left(\frac{E}{k_BT}\right)-1}, \quad (2b)$$

where n(E, T) and DW(T) are the Bose occupation factor and the Debye-Waller factor, respectively. $DW(T) = \exp(\langle u^2\rangle \cdot Q^2)$ is calculated, following a well established approach, from the $\langle u^2\rangle$ mean square displacements obtained with elastic scans performed *ad hoc* in the 5–100 K temperature range (data not shown), where the system is harmonic and $\langle u^2\rangle$ is linear with temperature, and assuming the same linear dependence at higher temperatures. As usual, the VDOS is divided by E^2 to enhance the excess contribution over the Debye level (reduced vibrational density of states, R-VDOS). The intensity, position, and variance of $g(E)/E^2$ are then calculated according to

$$M_0 = \int \frac{g(E)}{E^2}dE, \quad (3a)$$

$$M_1 = \frac{\int E\cdot\frac{g(E)}{E^2}dE}{M_0}, \quad (3b)$$

$$M_2 = \frac{\int E^2\cdot\frac{g(E)}{E^2}dE}{M_0} - M_1^2. \quad (3c)$$

III. RESULTS AND DISCUSSION

A. Inelastic neutron scattering

Typical spectra are reported in Figure 2. A vibrational excess centered at about 5 meV (BP) is clearly visible in the low temperature spectra where it emerges as a peak over the other

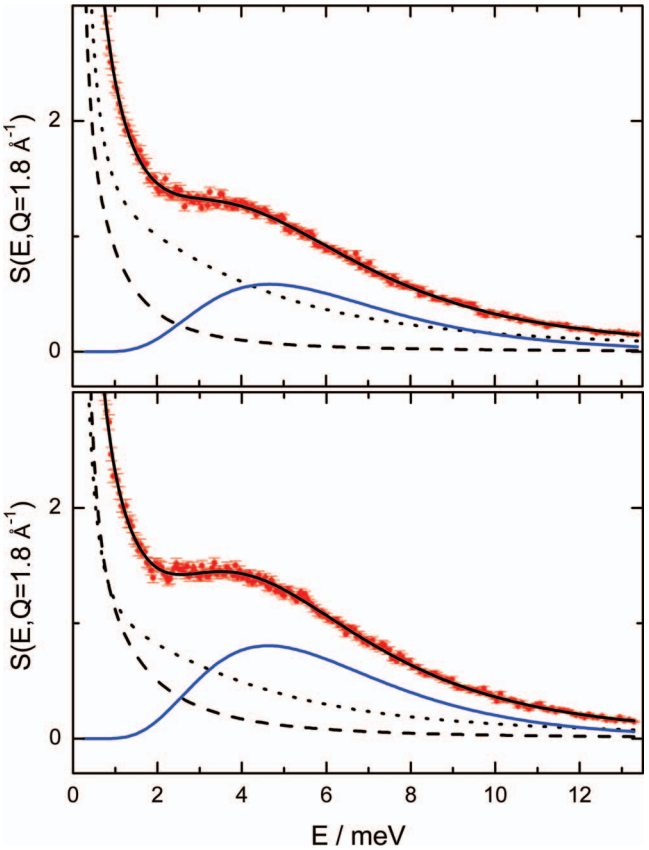

FIG. 3. Fit of inelastic spectra at T = 225 K for samples at h = 0.19 (upper panel) and h = 0.42 (lower panel). Circles (red): experimental data; dotted line: matrix contribution; dashed line: quasi-elastic contribution; and continuous line (blue): log-normal distribution representing the boson peak. The total fit is also reported as a continuous line superimposed to the experimental data.

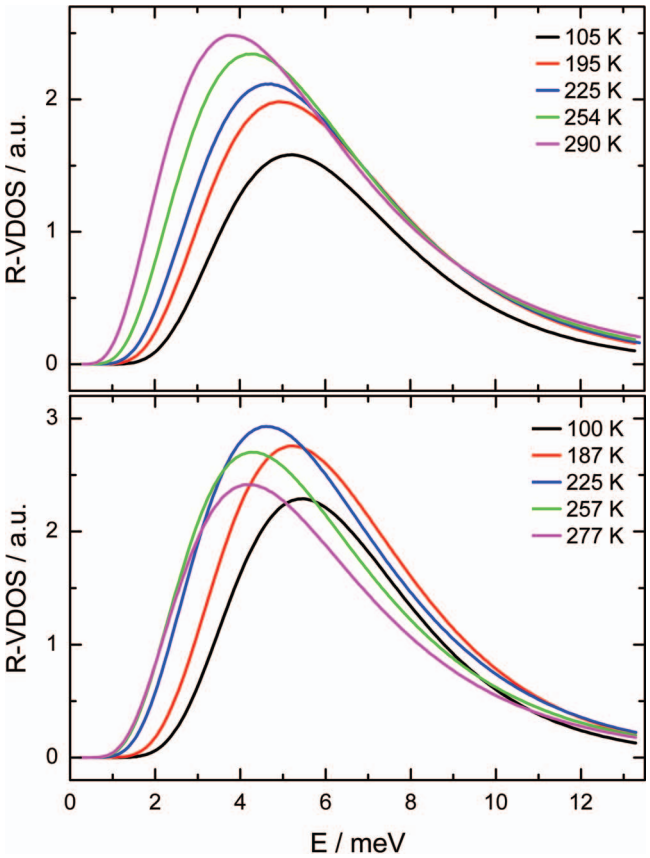

FIG. 4. R-VDOS as a function of energy at selected temperatures. (Upper panel) h = 0.19. (Lower panel) h = 0.42.

contributions; at temperatures higher than about 235 K the quasi elastic contribution grows in amplitude and width and almost smears out the boson peak that, at T ∼ 280 K, remains only as a barely visible shoulder. At low temperatures the boson peak is more evident in the h = 0.42 sample and this fact, together with its absence in the matrix spectra, indicates that it must be attributed to the water confined within the pores of the silica matrix. To obtain quantitative information on the temperature dependence of the BP we analyzed the data in terms of Eq. (1). Typical fits are reported in Figure 3; fits of analogous quality are obtained at all the temperatures investigated. As reported in Sec. II, from the lognormal distribution taking into account the inelastic contribution we obtain the VDOS (see Eqs. (2a) and (2b)); further division by E^2 to enhance the excess contribution over the Debye level yields the R-VDOS that is reported, at selected temperatures, in Figure 4. Some relevant features are already evident from visual inspection. In fact, R-VDOS redshifts and widens by increasing the temperature, the effect being similar for the two hydrations; conversely, the intensities behave in a different way: while for the sample at h = 0.19 they increase monotonically with temperature, for the sample at h = 0.42 an inversion is observed at about 225 K. More detailed information is obtained by calculating the R-VDOS zeroth, first, and second moments, following Eqs. (3a), (3b), and (3c); results are reported in Figure 5. Concerning the zeroth moment, the different hydration dependent behavior is striking: for the h = 0.42 sample a clear inversion is observed at 225 K so that at higher temperatures the BP area tends to vanish, while for the h = 0.19 sample a monotonous increase is observed. Concerning the position (M_1) and width (M_2) of the boson peak, no hydration effect is observed. Qualitatively, a BP redshift with temperature may be attributed to the effect of anharmonicity, while a BP widening may be attributed to the effect of mode damping. We note that redshift and widening of the R-VDOS with increasing temperature has been observed in the simulations of TIP4P/2005 supercooled water by Kumar *et al.*,[19] and that our low temperature M_1 value of ∼6 meV (∼50 cm^{-1}) is in very good agreement with their calculated value. We note also that around 225 K we observe a smooth temperature dependence of M_1 and M_2, in agreement with the results of a very recent study on the pressure and temperature dependence of the BP in deeply cooled water confined in MCM-41-S.[22] In that study, the authors state that the BP "emerges" if a maximum in the S(E, Q = 1.8 Å^{-1}) curve is observed between 2 and 10 meV; otherwise, the BP has "disappeared." With this semi-quantitative definition they obtain, in the temperature-pressure plane, an "emergence line" of the BP that, below 1600 bars, is parallel (although not coincident) with the so-called Widom line, defined as the line in the water phase diagram formed by the points of maxima of thermodynamic response functions; this behavior is taken as further evidence for a liquid-liquid crossover in deeply cooled confined

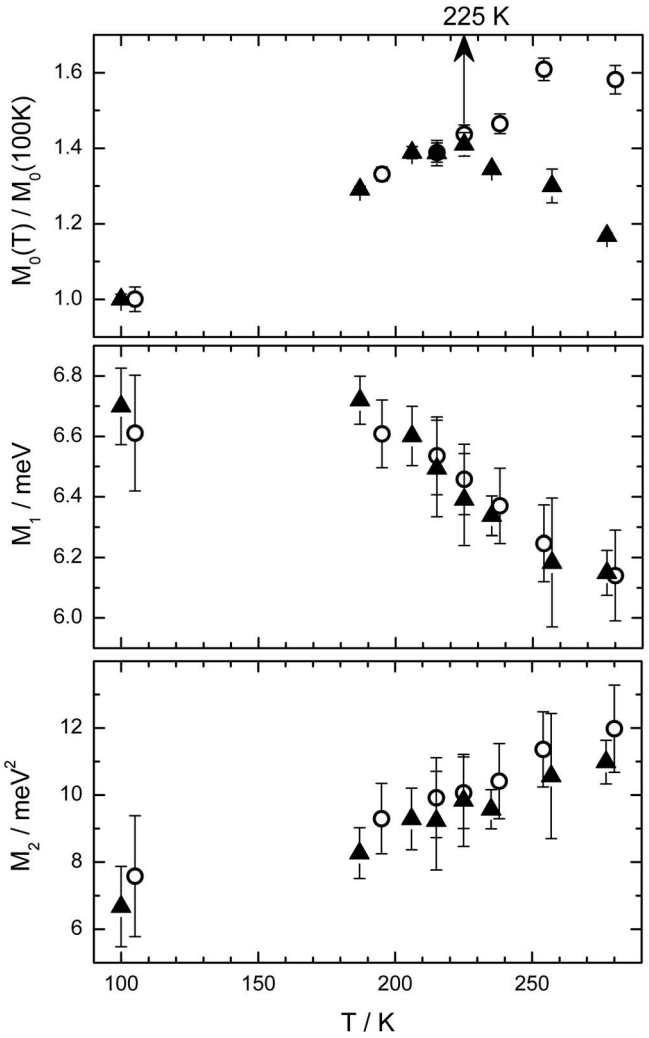

FIG. 5. Moments of the R-VDOS as a function of temperature at h = 0.19 (open circles) and h = 0.42 (full triangles). (Upper panel) Zero moments normalized to their low temperature values in order to take into account different sample composition and weight, (middle panel) first moment, and (lower panel) second moment.

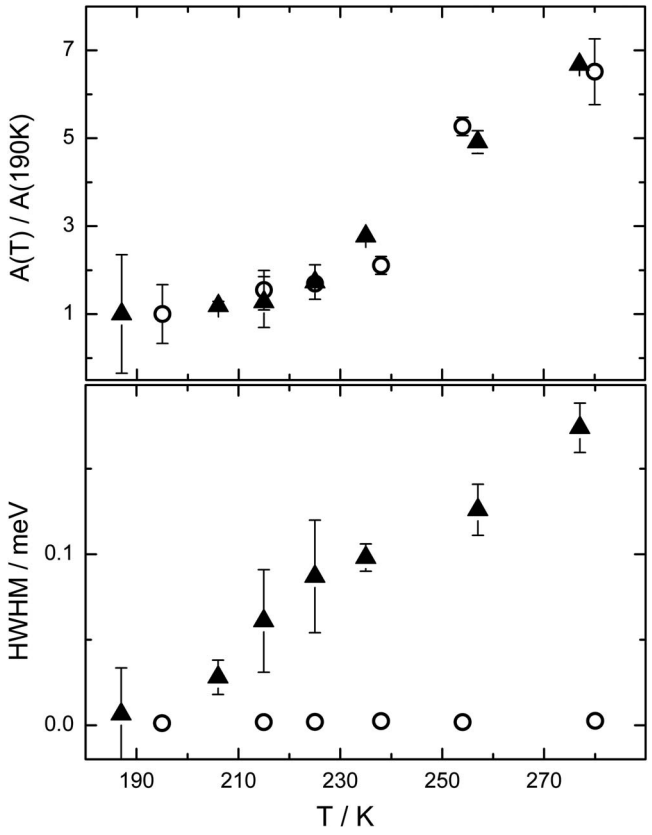

FIG. 6. Temperature dependence of the quasi-elastic contribution for h = 0.19 (open circles) and h = 0.42 (full triangles). (Upper panel) Normalized amplitude and (lower panel) half width.

water. It is important to stress that our data on normalized M_0 are in full agreement with this view since they highlight the presence of an inversion point at about 225 K, i.e., the temperature where a fragile-to-strong crossover is observed in the temperature dependence of relaxation times of nano-confined water[7] and in the protein hydration water.[12]

To check the validity of our BP results, the temperature dependence of the quasi-elastic contribution has to be investigated. Amplitudes and Half Widths at Half Maximun (HWHM) of the quasi-elastic contribution (sum of the L_1 and L_2 terms in Eq. (1)) are reported in Figure 6 as a function of temperature. As expected, an amplitude increase with temperature is observed; however, no hydration dependence is present, indicating that the M_0 inversion observed for the BP at h = 0.42 is not due to an anomalous increase of the quasi-elastic contribution but is a real property of the BP. Concerning the HWHM, we note that it is much smaller for the h = 0.19 sample, in agreement with the fact that water strongly interacting with pore walls moves on a lower time scale than internal water; moreover, its increase with temperature is barely visible in the ordinate scale of Figure 6. Concerning the h = 0.42 sample, the larger HWHM has to be attributed to internal water and its marked increase with temperature is expected; considering the rather large error bars, we prefer not to speculate about the possible presence of an inflection at about 225 K. A detailed analysis of QENS data on our samples will be given in a separate publication (Schirò *et al.*[31]).

B. Differential scanning calorimetry

In order to obtain information on the thermodynamic state of confined water studied with INS, we measured the calorimetric response in the temperature range 120–300 K, as described in Sec. II and also reported in Ref. 28. The results are reported in Figure 7, upper panel. As clearly highlighted by the derivative scans (Figure 7, lower panel), water confined in the silica xerogel at the hydration level h = 0.42 exhibits a second order-like transition (corresponding to the peak in the derivative thermogram) at about 170 K, followed by a first order-like endothermic transition (corresponding to the downward inflection in the derivative thermogram) at about 230 K. We note that no signs of crystallization (heat flow exothermic peak or upward inflection in the derivative thermogram) are present in between. The data in Figure 7 suggest that water confined within the pores of the silica xerogel matrix is a glass at temperatures below 173 K, where it undergoes a second order-like glass-liquid transition. At about

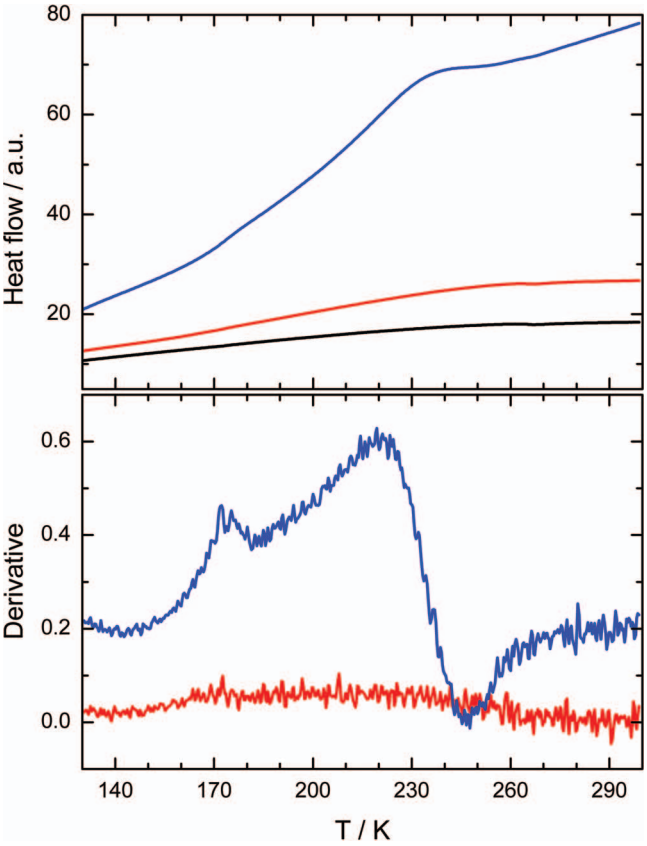

FIG. 7. (Upper panel) Calorimetric up-scans (scan rate 20 K/min) of silica xerogels at different hydration; from bottom to top: h = 0.05 (black), h = 0.19 (red), and h = 0.42 (blue). (Lower panel) Derivatives of hydrated samples up-scans after subtraction of the matrix contribution; red: h = 0.19 and blue: h = 0.42.

230 K, a first order-like liquid-liquid transition occurs. Analogous DSC data on the sample at hydration level h = 0.19 are also reported in Figure 7 and evidence the presence of a barely detectable broad glass transition at lower temperature with respect to h = 0.42 (in agreement with an already reported decrease of glass transition temperature in water strongly interacting with pores walls[29,30]). However, data do not show any sign of the first order-like transition detected in the sample at h = 0.42. A DSC scan on the "dry" sample (h = 0.05) is also shown in Figure 7 to characterize the calorimetric response of silica matrix and subtract it from the data on hydrated samples. The results reported in Figure 7 provide essential information on the thermodynamic state of water confined in the silica xerogel matrix and help understanding the INS results reported in Sec. III A. First of all, DSC data confirm that in the temperature range investigated by INS no crystallization occurs in the hydrated samples and water is in a liquid state at temperatures above 180 K. Moreover, and more important, DSC results perfectly parallel the results obtained by INS. At low hydration (h = 0.19), where a negligible quantity of "internal" water is present in the silica xerogel matrix, no sign of a liquid-liquid crossover is detected in the calorimetric scan and no inflection is revealed in the temperature dependence of BP intensity. Conversely, at higher hydration (h = 0.42), where the pores of the silica xerogel matrix are filled, a clear evidence of a liquid-liquid crossover is observed by DSC and, accordingly, an inversion in the trend of BP intensity is revealed at the same temperature (about 225 K). Note that even if the scenario proposed in Ref. 22 (in which deeply cooled confined water is, at ambient pressure, in a single liquid phase) is accepted, our calorimetric data clearly show a specific heat maximum at about 230 K; in this view the inversion point observed for the BP intensity should correspond to the crossing of the Widom line.

IV. CONCLUSIONS

In this work we presented the results of a thorough inelastic neutron scattering study on deeply cooled water confined in a disordered silica xerogel matrix to investigate the behavior of low-frequency modes of water (Boson peak) and its possible connection to the proposed liquid-liquid phase transition. The use of different hydration levels allowed us to exactly identify the contribution of internal water to neutron inelastic spectra and to reveal a clear inflection point in the Boson peak intensity at 225 K. Complementary differential scanning calorimetry data on the very same samples helped clarifying that what occurs at 225 K is a first order-like liquid-liquid crossover (or, more conservatively, a specific heat maximum). Our data provide a clear experimental evidence of the correlation between the presence and the behavior of Boson peak and the liquid-liquid crossover occurring in water at 225 K at ambient pressure, as recently proposed by molecular dynamics simulation of supercooled bulk water,[19] and in agreement with very recent experimental data on deeply cooled water confined in a MCM-41-S matrix.[22]

ACKNOWLEDGMENTS

The authors are indebted to T. Seydel for assistance during neutron scattering experiments at IN6 end station and to ILL for beamtime allocation.

[1]H. E. Stanley, P. Kumar, S. Han, M. G. Mazza, K. Stokeley, S. V. Buldyrev, G. Franzese, F. Mallamace, and L. Xu, J. Phys.: Condens. Matter **21**, 504105 (2009).
[2]F. Mallamace, C. Branca, M. Broccio, L. Corsaro, N. Gonzalez-Segredo, J. Spooren, H. E. Stanley, and S.-H. Chen, Eur. Phys. J. Spec. Topics **161**, 19 (2008).
[3]C. E. Bertrand, Y. Zhang, and S.-H. Chen, Phys. Chem. Chem. Phys. **15**, 721 (2013).
[4]M. G. Mazza, K. Stokeley, H. E. Stanley, and G. Franzese, J. Chem. Phys. **137**, 204502 (2012).
[5]P. H. Poole, F. Sciortino, U. Essmann, and H. E. Stanley, Nature (London) **360**, 324 (1992).
[6]J. C. Palmer, F. Martelli, Y. Liu, R. Car, A. Z. Panagiotopoulos, and P. G. Debenedetti, Nature (London) **510**, 385 (2014).
[7]L. Liu, S.-H. Chen, A. Faraone, C. W. Yen, and C. Y. Mou, Phys. Rev. Lett. **95**, 117802 (2005).
[8]S.-H. Chen, F. Mallamace, C. Y. Mou, M. Broccio, C. Corsaro, A. Faraone, and L. Liu, Proc. Natl. Acad. Sci. U.S.A. **103**, 12974 (2006).
[9]F. Mallamace, M. Broccio, C. Corsaro, A. Faraone, U. Wanderlingh, L. Liu, C. Y. Mou, and S.-H. Chen, J. Chem. Phys. **124**, 161102 (2006).
[10]J. M. Zanotti, M. C. Bellissent-Funel, and S.-H. Chen, Europhys. Lett. **71**, 91 (2005).
[11]P. Gallo, M. Rovere, and S.-H. Chen, J. Chem. Phys. Lett. **1**, 729 (2010).
[12]S.-H. Chen, L. Liu, X. Chu, Y. Zhang, E. Fratini, P. Baglioni, A. Faraone, and E. Mamontov, Proc. Natl. Acad. Sci. U.S.A. **103**, 9012 (2006).
[13]G. Schirò, M. Fomina, and A. Cupane, J. Chem. Phys. **139**, 121102 (2013).
[14]D. T. Limmer and D. Chandler, J. Chem. Phys. **135**, 134503 (2011).

[15]D. T. Limmer and D. Chandler, J. Chem. Phys. **138**, 214504 (2013).
[16]M. Vogel, Phys. Rev. Lett. **101**, 225701 (2008).
[17]S. Pawlus, S. Khodadadi, and A. P. Sokolov, Phys. Rev. Lett. **100**, 108103 (2008).
[18]J. A. Sellberg *et al.*, Nature (London) **510**, 381 (2014).
[19]P. Kumar, K. T. Wikfeldt, D. Schlesinger, L. G. M. Pettersson, and H. E. Stanley, Sci. Rep. **3**, 1980 (2013).
[20]S.-H. Chen, F. Mallamace, L. Liu, D. Z. Liu, X. Q. Chen, Y. Zhang, C. Kim, A. Faraone, C.-Y. Mou, E. Fratini, P. Baglioni, A. I. Kolesnikov, and V. Garcia-Sokoi, AIP Conf. Proc. **982**, 39 (2008).
[21]S.-H. Chen, Y. Zhang, M. Lagi, S. H. Chang, P. Baglioni, and F. Mallamace, J. Phys.: Condens. Matter **21**, 504102 (2009).
[22]Z. Wang, K.-H. Liu, P. Le, M. Li, W.-S. Chiang, J. B. Leão, J. R. D. Copley, M. Tyagi, A. Podlesnyak, A. I. Kolesnikov, C.-Y. Mou, and S.-H. Chen, Phys. Rev. Lett. **112**, 237802 (2014).
[23]A. Cupane, M. Levantino, and M. G. Santangelo, J. Phys. Chem. B **106**, 11323 (2002).
[24]M. Cammarata, M. Levantino, A. Cupane, A. Longo, A. Martorana, and F. Bruni, Eur. Phys. J. E **12**, S63 (2003).
[25]M. G. Santangelo, M. Levantino, A. Cupane, and G. Jeschke, J. Phys. Chem. B **112**, 15546 (2008).
[26]M. D'Amico, G. Schirò, A. Cupane, L. D'Alfonso, M. Leone, V. Militello, and V. Vetri, Langmuir **29**, 10238 (2013).
[27]V. K. Malinowsky, V. N. Novikov, and A. P. Sokolov, Phys. Lett. A **153**, 63 (1991).
[28]A. Cupane, M. Fomina, J. Peters, I. Piazza, and G. Schirò, "Experimental evidence for a liquid-liquid crossover in deeply cooled confined water" (unpublished).
[29]M. Oguni, S. Maruyama, K. Wakabayashi, and A. Nagoe, Chem. Asian J. **2**, 514 (2007).
[30]M. Oguni, Y. Kanke, A. Nagoe, and S. Namba, J. Phys. Chem. B **115**, 14023 (2011).
[31]G. Schirò *et al.*, "Diffusive dynamics of deeply cooled confined water" (unpublished).